Derivative thermo-analysis application to assess the cooling rate influence on the microstructure of Al-Si alloy cast

M. Krupiński [a,*], K. Labisz [a], L.A. Dobrzański [a], Z.M. Rdzawski [a,b]

[a] Division of Materials Processing Technology, Management and Computer Techniques in Materials Science, Institute of Engineering Materials and Biomaterials, Silesian University of Technology, ul. Konarskiego 18a, 44-100 Gliwice, Poland

[b] Institute of Non-Ferrous Metals, ul. Sowińskiego 5, 44-100 Gliwice, Poland

* Corresponding author: E-mail address: mariusz.krupinski@polsl.pl

Materials

ABSTRACT

Purpose: The application of the UMSA device (Universal Metallurgical Simulator and Analyzer) has allow to determine the liquidus/solidus thermal points of solidified alloy, as well the thermal points, where phase- or eutectic crystallisation occurs.

Design/methodology/approach: Investigations were performed using cast aluminium-silicon alloys, known as EN AC-4XXXX according to the PN-EN 1706:2001 standard. The solidification process was investigated using the metallurgical UMSA simulator connected to recording devices equipped with simulating cooling system. For the alloy microstructure investigation the optical microscope and transmission and scanning electron microscope with EDS equipment were used for evaluation of the chemical composition of the phases occurred in the investigated alloy.

Findings: Investigation of the interdependences occurred between phase morphology and cooling rate using thermo-analysis has given the main results.

Practical implications: In the metal casting industry the improvement of the quality of components depends mainly on proper control over the production parameters.

Originality/value: The performed investigations allow to determine the microstructure changes as well the derivative curves in comparison to the cooling rate applied for the alloy.

Keywords: Metallic alloys; Al-Si; Microstructure; Thermo derivative analysis

1. Introduction

Copper and magnesium addition enable to perform precipitation hardening of the multicomponent aluminium alloys with silicon, by precipitation of the Al_2Cu or Mg_2Si phase particles. However copper addition deteriorates corrosion resistance, which can be improved by 1% nickel addition. Copper addition up to 1% causes in the modified Al-Si-Mg alloys porosity enhancement when the copper addition exceed mass 0, 2%. Porosity enhancement is depending on the amount of big

inter-dendritic copper containing phases, which are solidified in a lower temperature compared to the Al-Si eutectic [1, 2, 3].

Mechanical properties of the Al-Si alloys are connected to the size, shape and distribution of the Si-eutectic present in the microstructure, because of the improvement of mechanical properties. These alloys are in general modified, for the reason of change of the fibrous Si phase morphology what makes it possible to achieve better mechanical properties of the Al-Si alloys. Not properly set casting temperature, unsuitable kind or mass concentration of the modifying additives influences also on the occurrence of undesirable microstructure being present after solidification [5].

To avoid such undesirable microstructure, but also to determine proper technological parameters the Al-Si alloys are pre-heated and cooled during the investigation process, following the thermo-derivative analysis performed afterwards.

Changes in the thermo-derivative curve with shifting of characteristic temperature points allow to assess the level of microstructure changes of the investigated alloys [3, 4, 5].

Because of crystallisation conditions the α+β eutectic structures can be divided into three basic types of hypo-eutectic and eutectic silumin structures, which contain pre-eutectic silicon crystals with the α phase, or the α phase only, as well the irregular plate shaped eutectic, which is characterized by a lower inter-dendritic space, pre-eutectic silicon crystals and α phase and fibrous like eutectic.

Cooling rate increase causes an enhancement of the crystallisation temperature of the α phase dendrites, it causes also an increase of the alloy overcooling level. Cooling rate increase is responsible also for a decrease of the recalescence temperature of the investigated alloy, what is a mass for grain sizes as well the SDAS (Secondary Dendrite Arm Spacing) decrease.

Performed investigations show that the cooling rate modifies Si precipitation and influences also on homogenizing of the All alloy. Obtained result for the highest applied cooling rate is comparable with the effect of alloy modification [3, 6].

Crystallization kinetic change is caused by appliance of different cooling rates and it influences also the crystallisation overcooling grade of the α solid solution, α+β eutectic, this can be stated in the microstructure change, as well in the change of the mechanical properties of the Al-Si-Cu aluminium cast alloys. Exact knowledge of the cooling rate influence of the sand casts on structure and temperature of the phase transformations during non-equilibrium crystallization allows to perform an optimisation of the production process. The above mentioned premises makes it possible to state, that the actually studying subject matter concerning crystallization kinetics of the Al-Si-Cu aluminium cast alloys, can be considered as up-to-date not only because of the scientifically point of view, but also for the reason of practically application of the elaborated results [7,8].

Crystallisation of the liquid alloy is going from the liquid state to the liquidus line that means - to the beginning of the crystallization. Next, it follows the crystallisation of the eutectics and intermetallic phases to the point where the alloy is solid - the solidus line according to equilibrium diagrams [9, 10].

For this reason on the crystallization curve, some characteristic inflexion points occur coming from exothermic or endothermic reactions of the crystallizing phase transformations. It is difficult to determine unequivocally the crystallization

temperature of the phases occurred on the crystallisation curve. The determination is possible using the first derivative curve of the cooling line in the function of time - that means using the differential ATD curve called also derivative curve [3, 11].

The general equation, describing (Table 1) the crystallisation function as a derivative of the crystallisation, is given as:

$$\frac{dT}{dt} = \frac{A}{m \cdot c_p} \cdot \alpha(t) \cdot (T - T_0) + \frac{K_K}{m \cdot c_p} \cdot \left(m \frac{dz}{dt} + z \frac{dm}{dt} \right) \qquad (1)$$

Table 1.
Description of the equation factors

Symbol	Descriptions
c_p	Heat capacity
m	Mass of the crystallised metal
T	Temperature at time dt
T_O	Environment temperature
A	Sampler surface
K_K	Crystallisation constant
z	Nucleus number

In real conditions the crystallization of the Al alloys shows departures of the crystallization process resulting from the Al-Si equilibrium diagram, which is a double system with an eutectic and limited solubility of the components in a solid state. The treason of these deviations is fir of all the considerably higher alloy crystallization, compared to this occurred in equilibrium conditions, but also the change in the initial alloy structure in the liquid state, caused by impurities, or specially added modificators for the reason of structure modification and morphology changes of the α+β eutectic or shifting of the characteristic equilibrium diagram temperature points, because of the pressure increase during the alloy crystallisation process [12,13].

The alloy crystallization process was investigated using the innovatory metallurgical simulator UMSA (Universal Metallurgical Simulator and Analyzer) equipped with the registration unit with model cooling system. UMSA is a unique device for recording the most important parameters relating to the solidification process. This device allows to determine the liquidus/solidus points of the crystallized alloy as well to determine the points, where the crystallisation of phase or eutectics occurs [14].

2. Materials and experimental procedure

Cast aluminium alloys of the AC-AlSi7Cu3Mg and AC-AlSi12CuNiMg type were used for investigations, the chemical composition of these alloys is presented was used in Table 1 and Table 2. The investigated alloys were cooled at a chosen cooling rate in the range of 0.2 to 1°C/s. The cooling rate was set as the range between the liquidus and solidus temperature point for the investigated alloys.

The cooling rate of ~0.2°C/s was achieved by applying free cooling, where increase of the cooling rate was obtained by compressed air injection into the sample chamber.

For statement of the interdependence between chemical composition and microstructure of the AC-AlSi7Cu3Mg and

AC-AlSi12CuNiMg (EN 1706:2001) aluminium cast alloys, cooled at different cooling rate, followed the investigations:

- alloy microstructure using MEF4A optical microscope supplied by Leica together with the image analysis software as well electron scanning microscope using Zeiss Supra 25 device within high resolution mode. The samples for optical microscope investigations were electro etched using 30% HBF_4.
- phase composition using EBSD and chemical composition of the Al alloy using qualitative and quantitative X-Ray analysis, as well EDS microanalysis,
- derivative thermo analysis using the UMSA thermo simulator (Fig. 1),
- hardness was measured using the Rockwell hardness tester supplied by Zwick ZHR 4150.

Table 2.
Chemical composition of the AC-AlSi7Cu3Mg aluminum alloy

Mass concentration of the element, in wt.%, AA standard			
Si	Cu	Mg	Mn
6.5-8	3-4	0.3-0.6	0.2-0.65
Fe	Ti	Zn	Ni
≤ 0.8	≤ 0.25	≤ 0.65	≤ 0.3

Table 3.
Chemical composition of the AC-AlSi12CuNiMg aluminum alloy

Mass concentration of the element, in wt.%, AA standard			
Si	Cu	Mg	Mn
10.5-13.5	0.8-1.5	0.8-1.5	0.35
Fe	Ti	Zn	Ni
0.6	0.2	0.35	0.35
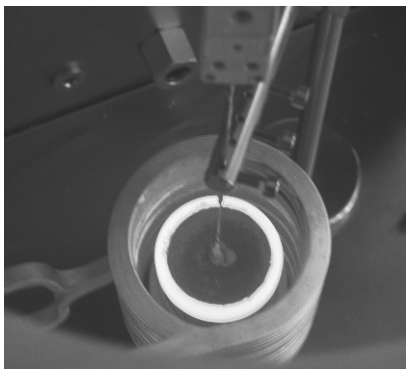
Fig. 1. Overview of the heating- and cooling system of the UMSA device

For measurement and recording of the temperature changes a K-type (chromo-alumel) thermocouples were used. Tests were performed several times for each cooling speed for statistical estimation of the investigation results.

The thermocouples were placed in the sample along to cylinder axes in the half distance of the cylinder generating line and its axis.

3. Results and discussion

As a result of the phase and chemical composition investigation of the cast aluminium alloy no difference in the chemical composition of the investigated alloys was stated. A difference in chemical composition could be caused by cooling rate change, chosen for the cooling process.

Cooling rate variations influence morphology changes of the precipitations occurred in the investigated alloys, basically the morphology of the β phase (#4). The effect of the cooling rate on the samples of the aluminium alloy causes microstructure refinement as well morphology change of the phases occurred, what was confirmed also by optical microscopy studies (Figs. 5-10). Investigations carried out reveal, that a significant Al_2Cu (#1) and Mg_2Si (#2) phase concentration occurs in a form of conglomerates, what is conformed to the crystallisation sequence ($\alpha+Al_2Cu+Mg_2Si+\beta$) of the phases and eutectics visible on the derivative curves. It was stated as a result of thin foil investigation on transmission electron microscope that the structure of the investigated alloys cooled at the applied cooling rates during the tests is mainly composed of Al_2Cu (Fig. 3) phase precipitations, with a morphology depending on copper mass concentration, as well on the cooling rate value. The performed EBSD (Electron Backscatter Diffraction) investigations with calculated Kikuchi lines confirm the occurrence of Mg_2Si (Fig. 2) phase and has not confirmed the preliminary results presented in this paper [15].

The chemical microanalysis investigations performed using the EDS electron depressive X-rays analysis on the scanning electron microscope has provide information about mass and atomic percentage concentration of particular elements in the point-wise investigated micro-areas of the aluminium matrix as well of the precipitations (Fig. 12-16). These investigations also, revel that the alloy is mainly composed of the following elements (#3): Al, Cu, Fe, Mn, Si and Mg. Also a variable copper concentration occurs inside the Al_2Cu phase particles, what is presented on the Fig. 11 in a form of white areas with fibrous morphology mainly in the middle of the Al_2Cu region.

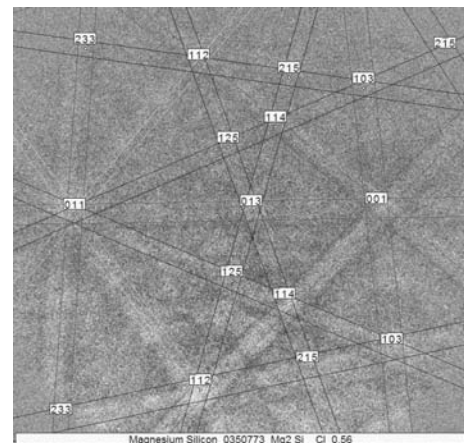The change of the cooling rate from 0.2 to 1°C/s causes an hardness increase of the investigated aluminium about ~17% (Fig. 4).
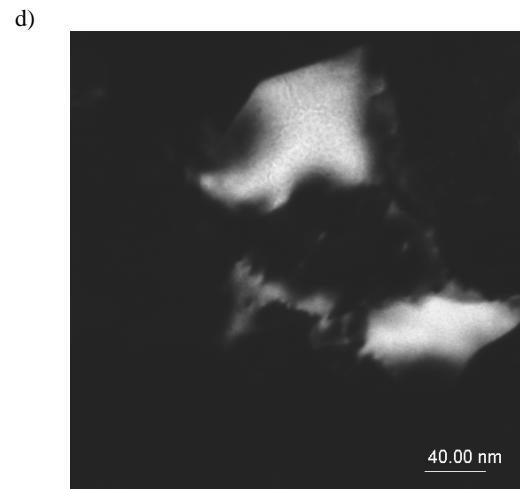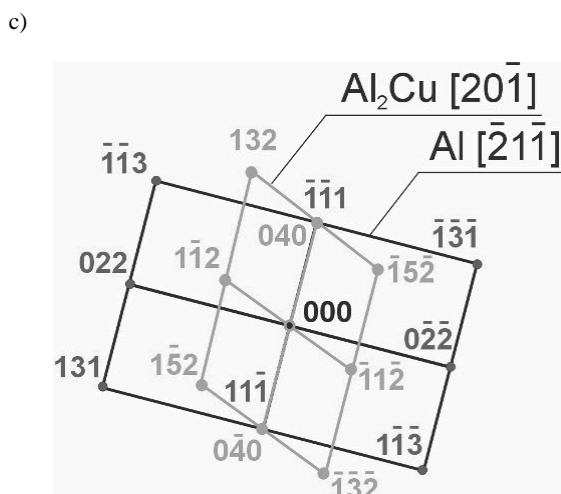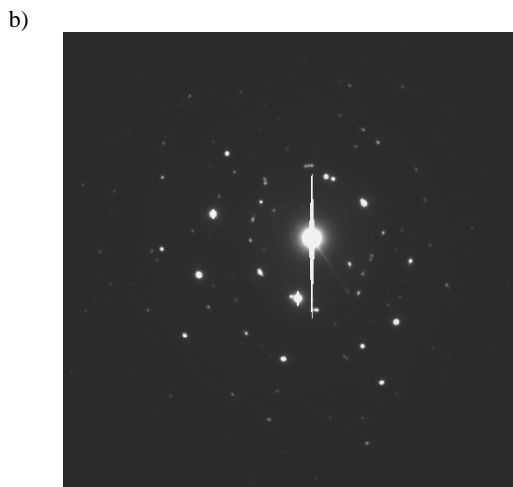

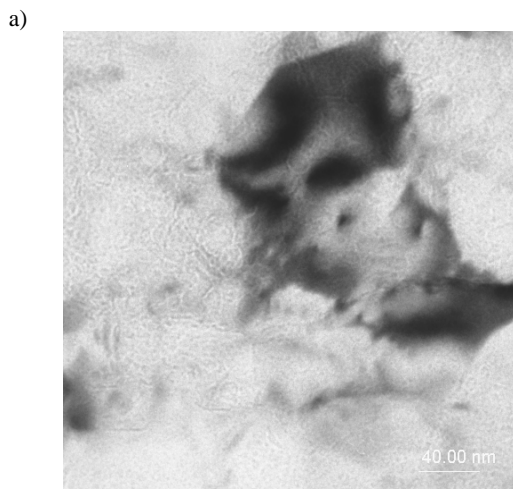Fig. 2. EBSD analysis result

a)

d)

b)

Fig. 3. TEM microstructures of the investigated thin foils, a) bright field image of the Al_2Cu phase, b) diffraction pattern of the phase, c) solution of the diffraction pattern, d) dark field image of the Al_2Cu phase particle.
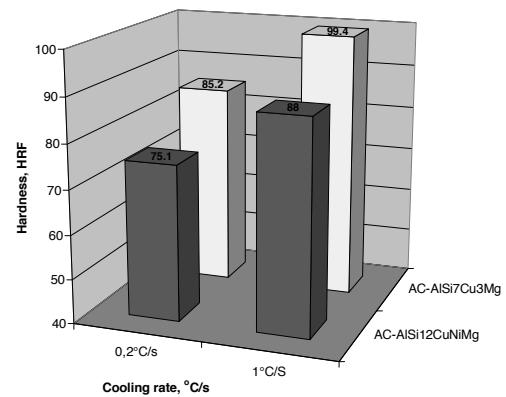

Fig. 4. Hardness vs. cooling rate dependence

c)

Initial temperature (T_{DN} - initial temperature of the α phase nuclei crystallisation) at the end of the crystallisation (T_{Sol} - temperature of the crystallisation end) was determined basing on the derivative curve (Fig. 17, 18) and the base line. Because of the crystallisation range both the curves have the same shape. Fraction solid was calculated using integral calculations, whereas the area below the derivative curve has been subtracted from the integral calculated area below the base line. The determined temperature of the beginning and the end of crystallisation at different cooling rates are showed in Table 4. The inflexion point of the fraction solid curve on Fig. 19 for the AC-AlSi7Cu3Mg alloy responds to the inflexion point of the derivative curve between the points of α phase and eutectic crystallisation. Increase of the cooling rate causes an over-cooling of the alloy, because for both of the alloys the T_{Sol} temperature is decreased about ~25°C for the AC-AlSi7Cu3Mg alloy and about ~15°C for the AC-AlSi12CuNiMg alloy as a result of cooling rate decrease of ~ 0.8 °C/s.

M. Krupiński, K. Labisz, L.A. Dobrzański, Z.M. Rdzawski

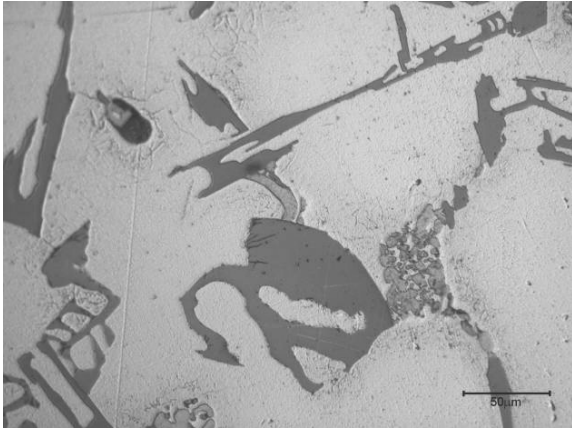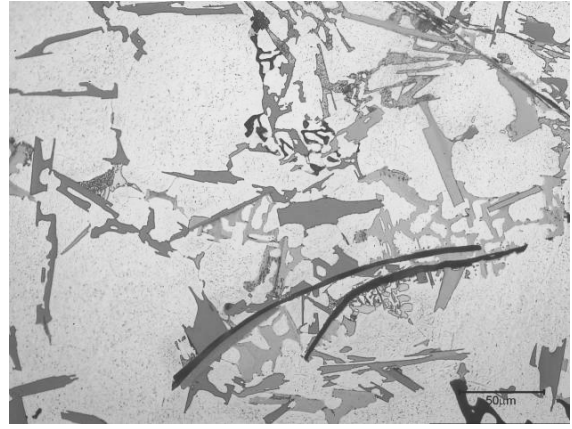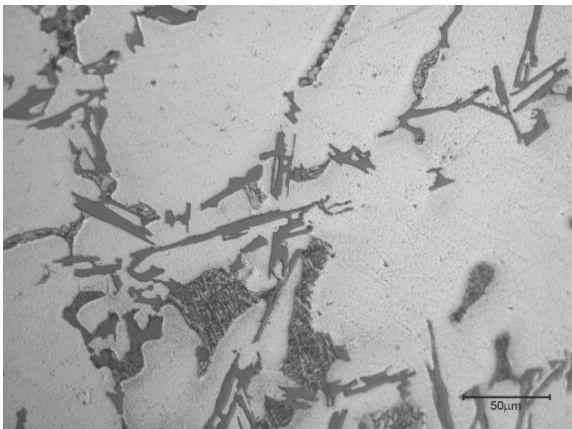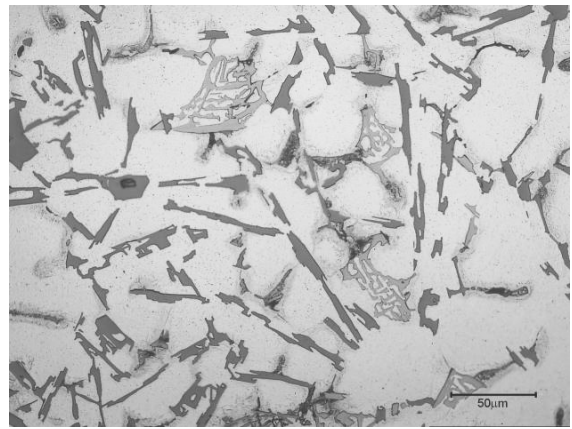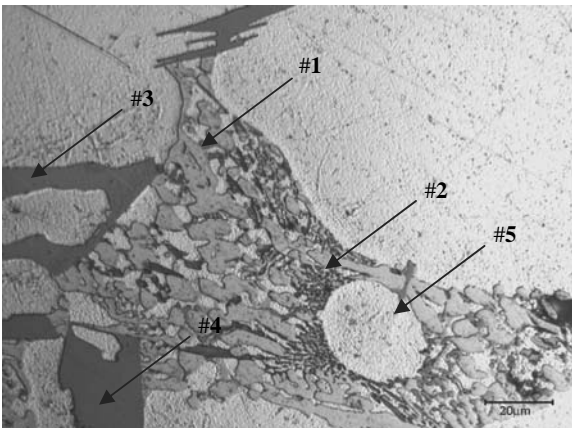Fig. 5. Optical micrograph of the AC-AlSi7Cu3Mg alloy, cylindrical sample, cooling rate ~0.2^{o}C/s

Fig. 8. Optical micrograph of the AC-AlSi12CuNiMg alloy, cylindrical sample, cooling rate ~0.2^{o}C/s

Fig. 6. Optical micrograph of the AC-AlSi7Cu3Mg alloy, cylindrical sample, cooling rate ~1°C/s

Fig. 9. Optical micrograph of the AC-AlSi12CuNiMg alloy, cylindrical sample, cooling rate ~1°C/s

Fig. 7. Optical micrograph of the AC-AlSi7Cu3Mg alloy, cylindrical sample, cooling rate ~0.2^{o}C/s
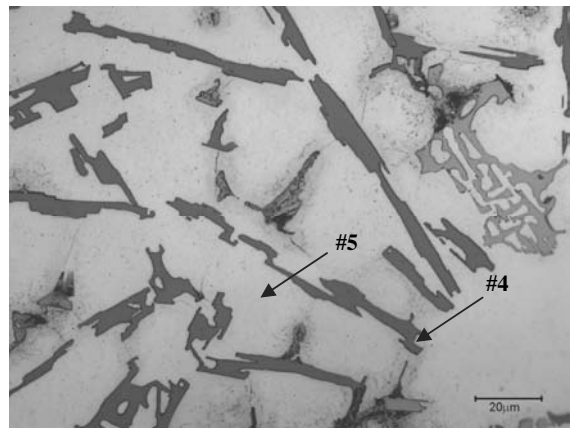
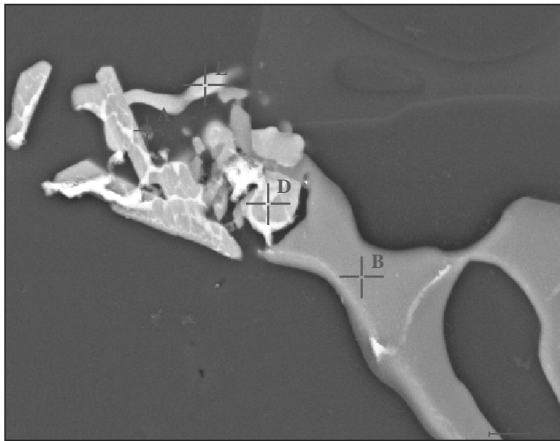Fig. 10. Optical micrograph of the AC-AlSi12CuNiMg alloy, cylindrical sample, cooling rate ~1°C/s

Fig. 11. SEM micrograph of the investigated AC-AlSi7Cu3Mg alloy
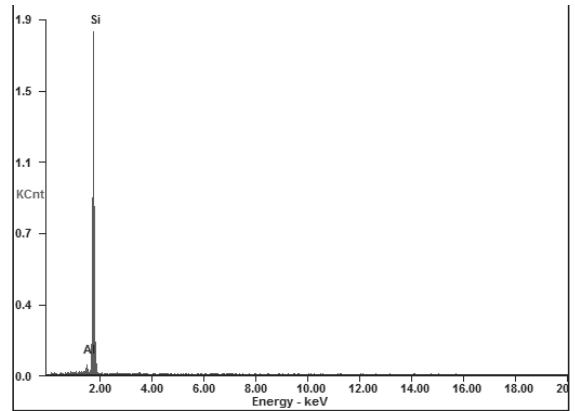

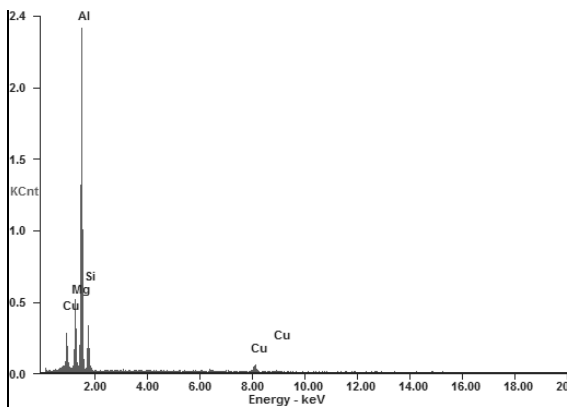Fig. 14. EDS pointwise analysis of the investigated aluminium cast alloy, marker C in Fig. 11

Fig. 12. EDS pointwise analysis of the investigated aluminium cast alloy, marker A in Fig. 11
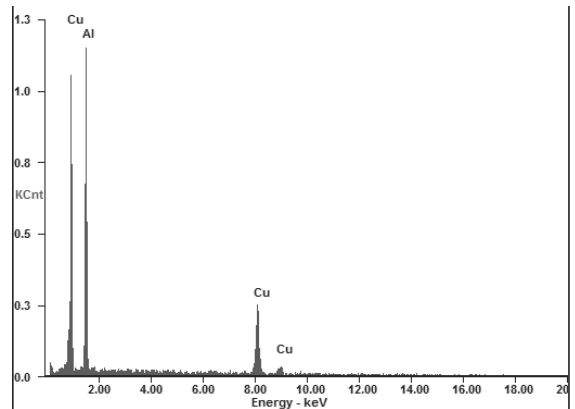

Fig. 15. EDS pointwise analysis of the investigated aluminium cast alloy, marker D in Fig. 11
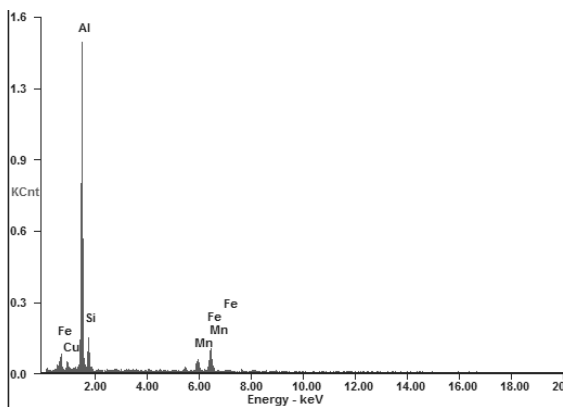

Fig. 13. EDS pointwise analysis of the investigated aluminium cast alloy, marker B in Fig. 11
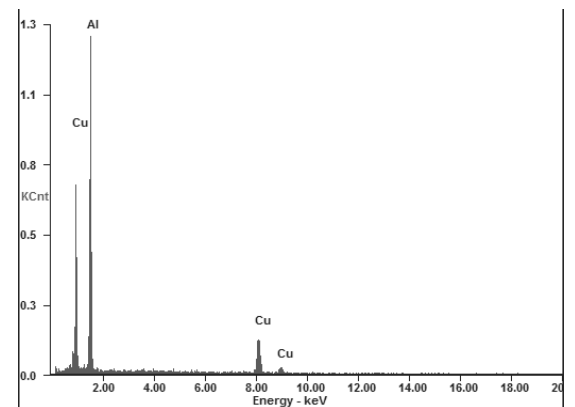

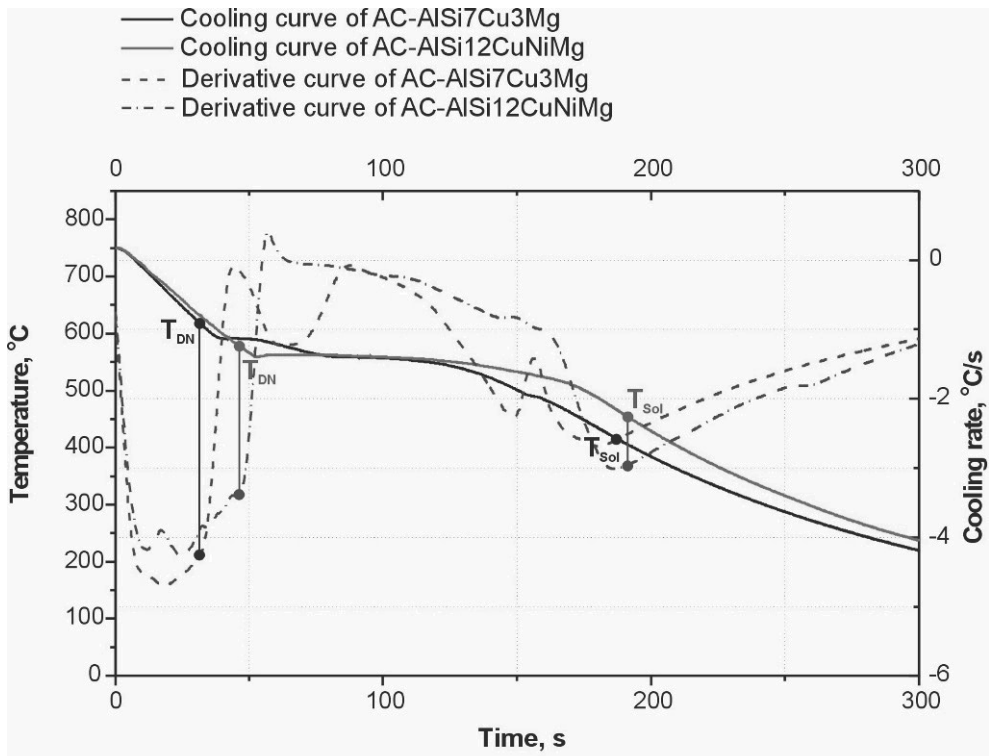Fig. 16. EDS pointwise analysis of the investigated aluminium cast alloy, marker E in Fig. 11

Fig. 17. Diagram of the cooling and derivative curves obtained for the investigated alloys at the cooling rate of ~1.0$^\text{o}$C/s

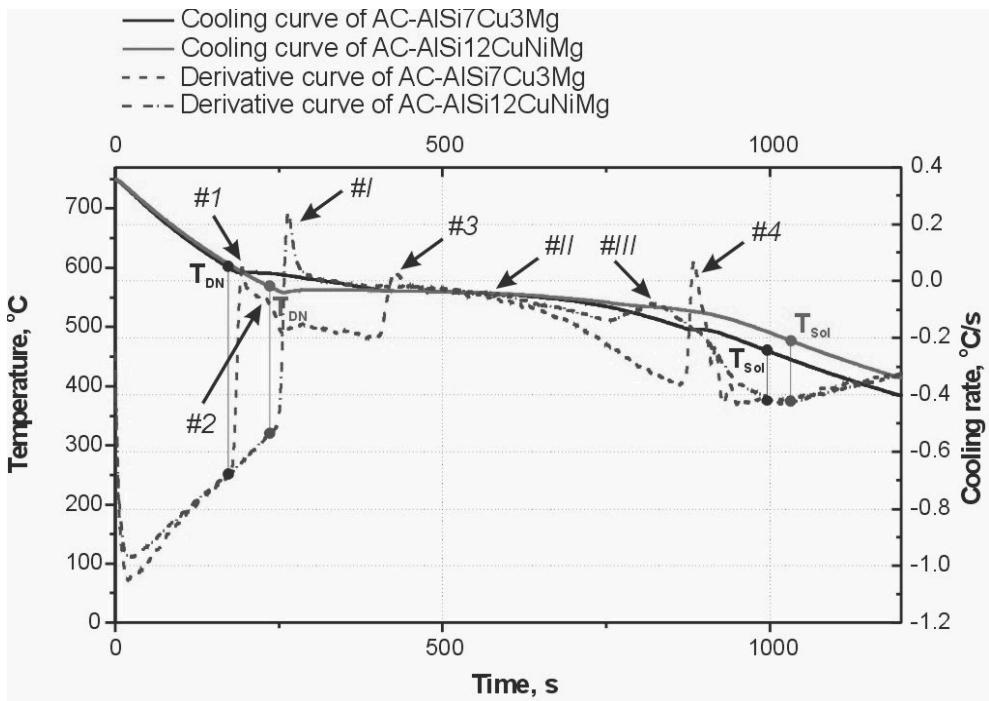Fig. 18. Diagram of the cooling and derivative curves obtained for the investigated alloys at the cooling rate of ~0.2$^\text{o}$C/s

Table 4.
T_{DN} and T_{Sol} solidification temperature

	AC-AlSi7Cu3Mg		AC-AlSi12CuNiMg	
	~0.2°C/s	~1°C/s	~0.2°C/s	~1°C/s
T_{DN}	598.77	619.92	590.65	596.74
T_{Sol}	448.32	423.40	483.15	469.00

T_{DN} - Initial temperature of crystallisation
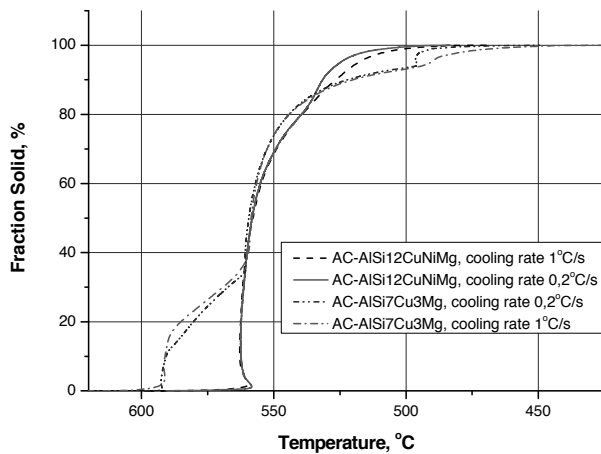T_{Sol} - Solid Temperature

Fig. 19. Fraction solid vs. temperature curve

Tab. 5 shows the crystallisation sequence of phases, eutectics and phases containing manganese iron and silicon manganese iron and silicon occurred in the investigated alloys, with the crystallisation ranges presented on the derivative curves (Fig. 18).

Table 5.
Description of the crystallisation sequence

Summary of reactions	Crystallisation points in Fig. 18
Al	#1
Al+AlFeMnSi	#2
Al+Si	#3
Al+Al₂Cu+Mg₂Si+Si	#4
Summary of reactions	Crystallisation points in Fig. 18
Al	#I
Al+Si+AlMnFeSi	#II
Al+Si+AlFeSi	#III

4. Conclusions

Investigations of an exact stoichiometric composition of the present phases allow to achieve better mechanical properties of the aluminium alloys as a result of conscious microstructure modelling. Cooling rate change of the investigated Al-Si alloys in the range of ~0.2 to ~1°C/s causes a phase morphology change, what can be seen on the derivative curves. Cooling rate increase by ~0.8°C/s causes microstructure refinement. Increase of the cooling rate of the AC-AlSi12CuNiMg alloy causes that the derivative curve reach the zero value only during the crystallisation of the α-phase matrix. Si

phase concentration increases up to the near-eutectic content according to the cooling and derivative curve as a result of a endothermic transformation of the α+β eutectic. The phase particles size depends on the cooling rate and shows a tight correlation to the derivative curve. Cooling rat change over a defined range causes microstructure changes and increases hardness at the same time.

References

[1] H. Mayer, M. Papakyriacou, B. Zettl, S.E. Stanzl-Tschegg, Influence of porosity on the fatigue limit of die cast magnesium and aluminium alloys, International Journal of Fatigue 25/3 (2003) 245-256.

[2] M. Wierzbińska, G. Mrówka-Nowotnik, Identification of phase composition of AlSi5Cu2Mg aluminium alloy in T6 condition, Archives of Materials Science and Engineering 30/2 (2008) 85-88.

[3] L. Bäckerud, G. Chai, J. Tamminen: Solidification Characteristics of Aluminum Alloys, Vol. 2., AFS, 1992.

[4] L. Bäckerud, G. Chai: Solidification Characteristics of Aluminum Alloys, Vol. 3, AFS, 1992.

[5] Q.G. Wang, Microstructural effects on the tensile and fracture behaviour of aluminum casting alloys A356/357, Metallurgical and Materials Transactions A 34/12 (2003) 2887-2899.

[6] D. Ovono, I. Guillot, D Massinon, The microstructure and precipitation kinetics of a cast aluminium alloy, Scripta Materialia 55/3 (2006) 259-262.

[7] M. Faraji, I. Todd, H. Jones, Effect of solidification cooling rate and phosphorus inoculation on number per unit volume of primary silicon particles in hypereutectic aluminium-silicon alloys, Journal of Materials Science 40/24 (2005) 6363-6365.

[8] S. Mudry, I. Shtablavyi, I. Shcherba, Liquid eutectic alloys as a cluster solutions, Archives of Materials Science and Engineering 34/1 (2008) 14-18.

[9] G. Pelayo, J.H. Sokołowski, R. Lashkari, A case reasoning aluminium thermal analysis platform for the prediction of W319 Al cast component characteristics, Journal of Achievements in Materials and Manufacturing Engineering 36/1 (2009) 7-17.

[10] H. Yamagata, H. Kurita, M. Aniołek, W. Kasprzak, J.H. Soko-lowski, Thermal and metallographic characteristics of the Al-20% Si high-pressure die-casting alloy for monolithic cylinder blocks, Journal of Materials Processing Technology 199 (2008) 84-90.

[11] Y. Birol, Analysis of macro segregation in twin-roll cast aluminium strips via solidification curves, Journal of Alloys and Compounds 486/1-2 (2009) 168-172.

[12] M. Krupiński, K. Labisz, L.A. Dobrzański, Z. Rdzawski, Derivative thermo analysis of the Al-Si cast alloy with addition of rare earths metals, Archieves of Foundry Engineering 10/1 (2010) 79-82.

[13] L.A. Dobrzański, M. Krupiński, K. Labisz, B. Krupińska, A Grajcar, Phases and structure characteristics of the near eutectic Al-Si-Cu alloy using derivative thermo analysis, Materials Science Forum 638-642 (2010) 475-480.

[14] L.A. Dobrzański, W. Kasprzak, M. Kasprzak, J.H. Sokolowski, A novel approach to the design and optimization of aluminum cast component heat treatment processes using advanced UMSA physical simulations, Journal of Achievements in Materials and Manufacturing Engineering 24/2 (2007) 139-142.

[15] M. Krupiński, K. Labisz, L.A. Dobrzański, Structure investigation of the Al-Si-Cu alloy using derivative thermo analysis, Journal of Achievements in Materials and Manufacturing Engineering 34/1 (2009) 47-54.